Deep Learning-based Energy Efficiency Maximization in Multi-STAR-RIS-Assisted Massive MIMO-NOMA Networks

Ridho Hendra Yoga Perdana* Toan-Van Nguyen[†], Yushintia Pramitarini*, Duy H. N. Nguyen[†], and Beongku An[‡]
*Dept. of Software and Communications Engineering in Graduate School, Hongik University, Republic of Korea

†Department of Electrical and Computer Engineering, San Diego State University, San Diego, CA, USA.

†Dept. of Software and Communications Engineering, Hongik University, Republic of Korea

Emails: mail.rhyp@gmail.com, vannguyentoan@gmail.com, yushintia@gmail.com,

duy.nguyen@sdsu.edu, beongku@hongik.ac.kr

Abstract—This paper studies deep learning (DL)-based energy efficiency maximization (EEM) in multi-simultaneous transmission and reflection-reconfigurable intelligent surfaces (STAR-RISs) assisted massive multiple-input multiple-output (mMIMO)non-orthogonal multiple access (NOMA) networks. We formulate the EEM problem to jointly optimize the precoding matrix and STAR-RIS phase shifts subject to the power budget at the base station, STAR-RIS phase shift constraints, and minimum quality-of-service (QoS) requirements. The formulated EEM problem belongs to the mixed-integer programming class, which is difficult to solve optimally. Thus, we develop an alternative optimization approach by dividing the original EEM problem into two sub-problems such as phase shift and beamforming optimization, and solve them alternatively. A bisection search algorithm is proposed to solve the phase shift optimization, while the inner approximation method is employed to address the non-convex beamforming problem through our newly tractable transformations. To enable real-time optimization, we design a DL framework that predicts optimal phase shifts and precoding matrices under various parameter settings. Simulation results demonstrate that the DL-based approach accurately predicts the optimal solutions and is significantly faster than conventional methods. We also evaluate the impact of the essential parameters on the system's performance.

Index Terms—CNN, energy efficiency, mMIMO, NOMA, non-convex optimization, phase shift, STAR-RIS.

I. Introduction

Massive multiple-input multiple-output (mMIMO) and non-orthogonal multiple access (NOMA) are key technologies for achieving high spectral efficiency (SE) [1] and energy efficiency (EE) [2] in the next-generation of wireless networks. However, as the number of users and antennas at the base station (BS) increases, the computational complexity of the resource allocation task also increases. To address this, deep learning (DL) has been extensively applied for tasks such as power allocation [3] and channel estimation [4] with fast processing times. Nonetheless, larger cell dimensions or obstacles between the BS and users can degrade signal quality. To solve this limitation, simultaneously transmitting and reflecting reconfigurable intelligent surfaces (STAR-RISs) have been introduced to extend coverage and enhance signal quality

by flexibly configuring their elements and supporting 360° coverage [5]. However, optimizing phase shifts is challenging due to the large number of STAR-RIS elements. To tackle this issue, a DL-based framework has been proposed to achieve optimal phase shifts in mMIMO-NOMA networks [1].

Leveraging the potential synergy of STAR-RIS, mMIMO-NOMA networks, and DL techniques, this paper focuses on maximizing EE in mMIMO-NOMA networks with multiple STAR-RISs to enhance signal quality at the users, followed by a DL-based framework for real-time resource allocation. The integration of DL and STAR-RIS within these networks offers improved system performance with low complexity and processing time. However, the impact of a combination of DL and STAR-RIS on addressing the EE problem in mMIMO-NOMA networks remains underexplored in existing research. Thus, we consider a downlink of multiple users in mMIMO-NOMA systems, where multiple STAR-RISs are deployed to assist the incident waves from the BS to the desired users. The main contributions of the paper are as follows:

- We formulate the energy efficiency maximization (EEM) subject to the minimum individual data rate, maximum power budget, and phase shift at the STAR-RIS constraints. Solving this problem is highly challenging since it involves non-linear mixed-integer programming.
- To address the formulated problem, we begin by relaxing the discrete variable (phase shift) into a continuous one and decomposing it into two sub-problems: beamforming and phase shift. We propose a bisection-based search algorithm to solve the phase shift sub-problem and the inner approximation method to handle the beamforming sub-problem.
- To enable real-time operation, we develop a DL framework using a CNN model to predict the optimal solution under the developed algorithm.
- Simulation results show that the EE improvement of the considered system, while the proposed DL-based framework accurately predicts the optimal solution to the

EEM problem as the conventional method but within a short execution time. Additionally, the impacts of the essential parameters are evaluated thoroughly.

Notation: a, \mathbf{A} , denote the scalar, vectors, and matrices, respectively. $\operatorname{diag}(\mathbf{A})$, $\|.\|$, $(.)^*$ are diagonal matrix, Euclidean norm of \mathbf{A} , complex comjugate, respectively. $\mathfrak R$ and $\mathbb C$ represent real part and complex numbers, respectively.

II. SYSTEM MODEL

A. System Description

We consider a downlink multi-users in multi-STAR-RIS-assisted mMIMO-NOMA networks as illustrated in Fig. 1, where a BS is deployed to serve simultaneously a set of near users $\mathcal{N} = \{\mathrm{UE}_n | n=1,...,N\}$ and a set of far users $\mathcal{F} = \{\mathrm{UE}_f | f=1,...,F\}$ via a set of STAR-RISs $\mathcal{K} = \{\mathrm{SR}_k | k=1,...,K\}$ using NOMA transmission. The BS, UE_n, and UE_f

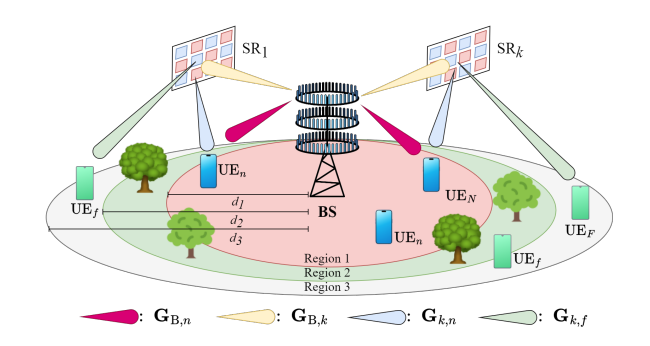


Fig. 1. The considered multi-STAR-RIS mMIMO-NOMA system.

are equipped with $M_{\rm BS}>1$, $M_n>1$, and $M_f>1$ antennas, respectively. We consider mode switching (MS) at the STAR-RIS, where it is equipped with $M_r^{\rm tr}+M_r^{\rm rf}=M_r$ passive elements allocating $M_r^{\rm tr}$ for transmission and $M_r^{\rm rf}=M_r$ for reflecting parts [6]. We assume the considered cell is divided into three regions virtually, where BS is deployed in the center of the cell. UE_n and UE_f are deployed randomly at region 1 and region 3, while the STAR-RIS is deployed randomly at the edge of the region 1. In the considered system, only UE_n has direct communication to BS, whereas no direct communication between BS to UE_f since natural obstacles in the region 2. It should be noted that UE_n has better channel condition than UE_f since UE_n has two communication links.

B. STAR-RIS-assisted mMIMO

The BS transmits the signal \mathbf{x} to UE_n and UE_f , which can be written as $\mathbf{x} = \sum_{n \in N} \mathbf{W}_n x_n + \sum_{f \in F} \mathbf{W}_f x_f$, where $\mathbf{W}_n \in \mathbb{C}^{M_{\mathrm{BS}} \times d}$ and $\mathbf{W}_f \in \mathbb{C}^{M_{\mathrm{BS}} \times d}$ are the linear precoding from BS to UE_n and UE_f , respectively, $x_n \in \mathbb{C}^{d \times 1}$ and $x_f \in \mathbb{C}^{d \times 1}$ with $1 \leq d \leq \min\{M_{\mathrm{BS}}, M_n, M_f\}$ are the data information for UE_n and UE_f , respectively. We define $\mathbf{W}_1 \triangleq [\mathbf{W}_n]_{n \in \mathcal{N}}, \ \mathbf{W}_2 \triangleq [\mathbf{W}_f]_{f \in \mathcal{F}},$ and $\mathbf{W} \triangleq [\mathbf{W}_1 \mathbf{W}_2]$ to simplify the notation.

The equivalent channel gains between the BS and UE_n , denoted by $\hat{\mathbf{G}}_n(\Phi)$, and BS and UE_f , denoted by $\hat{\mathbf{G}}_f(\Psi)$, are expressed, respectively, as

$$\hat{\mathbf{G}}_n(\mathbf{\Phi}) = \mathbf{G}_{\mathrm{B},n} + \sum_{k \in \mathcal{K}} \mathbf{G}_{\mathrm{B},k} \mathbf{\Phi}_k \mathbf{G}_{k,n}, \tag{1}$$

$$\hat{\mathbf{G}}_f(\mathbf{\Psi}) = \sum_{k \in \mathcal{K}} \mathbf{G}_{\mathrm{B},k} \mathbf{\Psi}_k \mathbf{G}_{k,f}, \tag{2}$$

where $\mathbf{G}_{\mathrm{B},n} \in \mathbb{C}^{M_n \times M_{\mathrm{BS}}}$ is channel gain from BS to UE_n , $\mathbf{G}_{\mathrm{B},k} \in \mathbb{C}^{M_r^{\mathrm{rf}} imes M_{\mathrm{BS}}}$ is channel gain from BS to SR_k with reflection/transmission part, $\mathbf{G}_{k,n} \in \mathbb{C}^{M_n \times M_r^{\mathrm{rf}}}$ is channel gain from SR_k with reflection part to UE_n and $\mathbf{G}_{k,f} \in \mathbb{C}^{M_f \times M_r^{\mathrm{tr}}}$ is channel gain from SR_k with transmission part to UE_f . The Φ is the phase shift matrix of SR_k with diagonal reflection matrix being $\Phi = \operatorname{diag}(\alpha_1 \phi_1, \cdots, \alpha_{M_r^{\mathrm{rf}}} \phi_{M_r^{\mathrm{rf}}}),$ where $\alpha_{m_r^{\rm rf}}\phi_{m_r^{\rm rf}}=e^{j\theta_{k,M_r^{\rm rf}}}$ with $\theta_{k,M_r^{\rm rf}}\in(0,2\pi]$ and Ψ is the phase shift matrix of SR_k with diagonal transmission matrix being $\Psi = \operatorname{diag}(\alpha_1 \psi_1, \cdots, \alpha_{M_n^{\operatorname{tr}}} \psi_{M_n^{\operatorname{tr}}})$, where $\alpha_{m_r^{\rm tr}}\psi_{m_r^{\rm tr}} = e^{j\theta_{k,M_r^{\rm tr}}}$ with $\theta_{k,M_r^{\rm tr}} \in (0,2\pi]$, while α is phase shift amplitude of reflection/transmission. In this paper, we consider the phase shift amplitude to be maximum (i.e., $\alpha_{m^{\rm rf}} = \alpha_{m^{\rm tr}} = 1$). And also, we consider the phase shift of transmission/reflection at each element of the STAR-RIS that is a discrete values so that the number of phase shifts is subject to the phase shift resolution. Then, the resolution of the phase shift at each STAR-RIS can be written as $\eta = 2^b$, where b is the number of bits used to quantize the number of phase shift levels [7]. Consequently, a set of discrete phase shift values at each element can be expressed as

$$Q = \{0, \delta\lambda, \cdots, (\eta - 1)\delta\lambda\},\tag{3}$$

where $\delta\lambda=2\pi/\eta$ with $\lambda=\{\phi,\psi\}$. The channel coefficient matrix $\mathbf{G}=\sqrt{\rho_g}\tilde{\mathbf{G}}$, $\tilde{\mathbf{G}}\in\{\mathbf{G}_{\mathrm{B},n},\mathbf{G}_{\mathrm{B},k},\mathbf{G}_{k,n},\mathbf{G}_{k,f}\}$, where ρ_g and $\tilde{\mathbf{G}}$ denote the large-scale and small-scale fadings, respectively.

The signal received by UE_n and UE_f can be expressed, respectively, as $\mathbf{y}_n = \hat{\mathbf{G}}_n(\Phi)\mathbf{W}_nx_n + \sum_{n'\in\mathcal{N}\setminus\{n\}}\hat{\mathbf{G}}_n(\Phi)\mathbf{W}_{n'}x_{n'} + \sum_{f\in\mathcal{F}}\hat{\mathbf{G}}_f(\Phi)\mathbf{W}_fx_f + \mathbf{n}_n$, $\mathbf{y}_f = \hat{\mathbf{G}}_f(\Psi)\mathbf{W}_fx_f + \sum_{f'\in\mathcal{F}\setminus\{f\}}\hat{\mathbf{G}}_f(\Psi)\mathbf{W}_{f'}x_{n'} + \sum_{n\in\mathcal{N}}\hat{\mathbf{G}}_n(\Psi)\mathbf{W}_nx_n + \mathbf{n}_f$, where \mathbf{n}_n and \mathbf{n}_f are additive white Gaussian noise at UE_n and UE_f , respectively, where $\mathbf{n} \sim \mathcal{CN}(\mathbf{0},\mathbf{I}\sigma^2)$ with $\sigma^2 \in \{\sigma_n^2,\sigma_f^2\}$ and zero mean. From the NOMA principle, the SINR at UE_n to subtract the UE_f signal using successive interference cancellation (SIC) can be expressed as

$$\gamma_n^{x_f}(\mathbf{W}, \mathbf{\Phi}) = \frac{\|\hat{\mathbf{G}}_n(\mathbf{\Phi})\mathbf{W}_f\|^2}{\Xi_{n,f}(\mathbf{W}, \mathbf{\Phi})},\tag{4}$$

where $\Xi_{n,f}(\mathbf{W}, \mathbf{\Phi}) = \sum_{f' \in \mathcal{F} \setminus \{f\}} \|\hat{\mathbf{G}}_n(\mathbf{\Phi}) \mathbf{W}_{f'}\|^2 + \sum_{n \in \mathcal{N}} \|\hat{\mathbf{G}}_n(\mathbf{\Phi}) \mathbf{W}_n\|^2 + \sigma_n^2$. Then, the SINR of UE_n to decode its own signal as

$$\gamma_n^{x_n}(\mathbf{W}, \mathbf{\Phi}) = \frac{\|\hat{\mathbf{G}}_n(\mathbf{\Phi})\mathbf{W}_n\|^2}{\Xi_{n,n}(\mathbf{W}, \mathbf{\Phi})},$$
 (5)

where $\Xi_{n,n}(\mathbf{W}, \mathbf{\Phi}) = \sum_{f \in \mathcal{F}} \|\hat{\mathbf{G}}_n(\mathbf{\Phi}) \mathbf{W}_f\|^2 +$

 $\sum_{n' \in \mathcal{N} \setminus \{n\}} \|\hat{\mathbf{G}}_n(\mathbf{\Phi}) \mathbf{W}_{n'}\|^2 + \sigma_n^2$. Different from UE_n , UE_f can decode its own signal directly yielding a SINR as

$$\gamma_f^{x_f}(\mathbf{W}, \mathbf{\Psi}) = \frac{\|\hat{\mathbf{G}}_f(\mathbf{\Psi})\mathbf{W}_f\|^2}{\Xi_{f,f}(\mathbf{W}, \mathbf{\Psi})},\tag{6}$$

where $\Xi_{f,f}(\mathbf{W}, \mathbf{\Psi}) = \sum_{f' \in \mathcal{F} \setminus \{f\}} \|\hat{\mathbf{G}}_n(\mathbf{\Phi}) \mathbf{W}_{f'}\|^2 + \sum_{n \in \mathcal{N}} \|\hat{\mathbf{G}}_n(\mathbf{\Phi}) \mathbf{W}_{n'}\|^2 + \sigma_n^2$. The downlink SE of UE_n and UE_f in nat/sec/Hz can be expressed, respectively, as

$$\mathcal{R}_n(\mathbf{W}, \mathbf{\Phi}) = \ln(1 + \gamma_n^{x_n}(\mathbf{W}, \mathbf{\Phi})), \quad \forall n \in \mathcal{N},$$
 (7)

$$\mathcal{R}_f(\mathbf{W}, \mathbf{\Psi}) = \ln(1 + \gamma_f^{x_f}(\mathbf{W}, \mathbf{\Psi})), \quad \forall f \in \mathcal{F}.$$
 (8)

C. Energy Efficiency Maximization

The main goal of this paper is to maximize the EE performance in the considered system subject to individual SE, maximum power budget at BS, and phase shift at STAR-RIS constraints. To obtain the EE, we consider the total hardware power consumption of the system as

$$\tilde{P} = (\|\mathbf{W}_{1}\|^{2} + \|\mathbf{W}_{2}\|^{2})\epsilon^{-1} + M_{BS}P_{BS}^{dyn} + P_{BS}^{stat} + M_{r}P_{r}^{stat} + \sum_{n \in \mathcal{N}} M_{n}P_{n}^{stat} + \sum_{f \in \mathcal{F}} M_{f}P_{f}^{stat}, \quad (9)$$

where $\epsilon \in (0,1]$ represents transmit power efficiency, P_{BS}^{dyn} denote the dynamic power consumption at BS, which correlates to the power radiation of all circuits in each active radio-frequency chain, P_{BS}^{stat} is the static power at BS used for a cooling system, while P_r^{stat} , P_n^{stat} , and P_f^{stat} denote the hardware static power at SR_r , UE_n , and UE_f , respectively. Then, we denote the total power circuit in the system as $P_{\Sigma}^{crt} = M_{\mathrm{BS}}P_{\mathrm{BS}}^{dyn} + P_{\mathrm{BS}}^{stat} + M_rP_r^{stat} + \sum_{n \in \mathcal{N}} M_nP_n^{stat} + \sum_{f \in \mathcal{F}} M_fP_f^{stat}$. Therefore, the EEM can be formulated as

P1: Original Problem

$$\max_{\mathbf{W}, \mathbf{\Phi}, \mathbf{\Psi}} \quad \text{EEM}_{\sum} \triangleq \frac{\sum_{n \in \mathcal{N}} \mathcal{R}_n(\mathbf{W}, \mathbf{\Phi}) + \sum_{f \in \mathcal{F}} \mathcal{R}_f(\mathbf{W}, \mathbf{\Psi})}{(\|\mathbf{W}_1\|^2 + \|\mathbf{W}_2\|^2)\epsilon^{-1} + P_{\sum}^{crt}}$$
(10a)

s.t.
$$\mathcal{R}_n(\mathbf{W}, \mathbf{\Phi}) \ge \bar{\mathsf{R}}_n, \quad \forall n \in \mathcal{N},$$
 (10b)

$$\mathcal{R}_f(\mathbf{W}, \mathbf{\Psi}) \ge \bar{\mathsf{R}}_f, \quad \forall f \in \mathcal{F},$$
 (10c)

$$||\mathbf{W}_n||^2 + ||\mathbf{W}_f||^2 \le \bar{P}_{BS},$$
 (10d)

$$\phi_{m_r^{\rm rf}} \in \mathcal{Q}, \quad \psi_{m_r^{\rm tr}} \in \mathcal{Q},$$
 (10e)

$$\alpha_{m_r^{\rm rf}} + \alpha_{m_r^{\rm tr}} = 1, \tag{10f}$$

$$\alpha_{m^{\text{rf}}} \in \{0, 1\}, \quad \alpha_{m_{-}^{\text{tr}}} \in \{0, 1\},$$
 (10g)

where constraints (10b) and (10c) are the QoS for the SE of UE_n and UE_f must be greater than the pre-defined minimum requirement $\bar{R}_n \geq 0$ and $\bar{R}_f \geq 0$, respectively. Constraint (10d) indicates the total power of all users in the system that must be less than equal to the maximum power budget at BS. Constraint (10e) indicates the phase shift at STAR-RIS that has a discrete value. Constraints (10f) and (10g) represent the MS working criteria of STAR-RIS, which is restricted to a binary value. Thus, it is clear that the objective function in (15a) is non-convex with respect to W_1 , W_2 , Φ and Ψ is belonging to the class of mixed-integer non-

convex programming class, which presents very challenges in finding its optimal solution.

III. THE PROPOSED EEM ALGORITHM

Actually, solving problem (10) is more complex than the spectral efficiency problem in [1] since the EEM is mixed integer non-convex fraction programming, which requires exponential complexity in finding its optimal solution. Nonetheless, we will show that the proposed algorithm based on the IA method can efficiently solve the formulated EEM problem through our transformations. One of the techniques to address the discrete property is by relaxing it to a continuous one. Thus, the relaxed form of problem (10) can be approximated as

P2: Relaxed

$$\max_{\mathbf{W}, \mathbf{\Phi}, \mathbf{\Psi}} \text{ EEM}_{\sum} \triangleq \frac{\sum_{n \in \mathcal{N}} \mathcal{R}_n(\mathbf{W}, \mathbf{\Phi}) + \sum_{f \in \mathcal{F}} \mathcal{R}_f(\mathbf{W}, \mathbf{\Psi})}{(\|\mathbf{W}_1\|^2 + \|\mathbf{W}_2\|^2)\epsilon^{-1} + P_{\sum}^{crt}}$$
(11a)

s.t.
$$\phi_{m_n^{\text{rf}}} \in (0, 2\pi],$$
 (11b)

$$(10b), (10c), (10d), (10f), (10g).$$
 (11c)

It should be noted that the problem (11) is fractional form and non-convex. To address this problem, we decouple problem (11) into phase shift optimization and beamforming optimization sub-problems and then address them alternatively.

A. Phase Shift Optimization Sub-Problem

In this paper, we address the phase shift optimization sub-problem by fixing the beamforming variable. Thus, the problem (11) can be re-expressed as

P3: Phase Shift:

$$\max_{\mathbf{\Phi}, \mathbf{\Psi}} \text{EEM}_{\Sigma} \triangleq \frac{\sum_{n \in \mathcal{N}} \mathcal{R}_n(\mathbf{\Phi})}{(N+F)\epsilon^{-1} + P_{\Sigma}^{crt}} + \frac{\sum_{f \in \mathcal{F}} \mathcal{R}_f(\mathbf{\Psi})}{(N+F)\epsilon^{-1} + P_{\Sigma}^{crt}}$$
(12a)

s.t.
$$(10b), (10c), (10f), (10g), (11b).$$
 (12b)

It can be shown that in the problem (12) the objective function (12a) is concave while constraint (11b) is a linear constraint. To address this problem efficiently, we propose a Bisection Search Algorithm-based approach in Alg. 1.

Algorithm 1 The Proposed Bisection Search algorithm to Solve sub-Problem (12)

Input: k, l.

Output: Φ_k^{\star} , Ψ_k^{\star} .

Initialize the lower and upper bounds of ϕ and ψ ;

- 1: repeat
- 2: Calculate $\phi^* = (\phi^{L} + \phi^{U})/2$; $\psi^* = (\psi^{L} + \psi^{U})/2$
- 3: Update $\phi_{m_{\underline{r}f}}(\phi^{\star})$; $\psi_{m_{\underline{r}f}}(\psi^{\star})$
- 4: Solve the problem (12);
- 5: until Convergence

It should be noted that since the optimal solution of phase shift is continuous values, it cannot be directly applied to the originally formulated problem. To address this issue, we introduce the round function to the problem (12) after achieving the optimal values as

$$\boldsymbol{\xi}^{\star} = [\boldsymbol{\xi}^{(\star)} + \Delta], \ \forall k \in \mathcal{K}, \tag{13}$$

where $\boldsymbol{\xi}^{(\star)} \in \{\boldsymbol{\Phi}_k^{\star}, \boldsymbol{\Psi}_k^{\star}\}$, and $\Delta = (360/\eta)/2$ is the rounding step size. Once we achieve the optimal phase shift values, the beamforming optimization sub-problem will be solved alternately, which will be explained in the following subsection.

B. Beamforming Optimization Sub-Problem

Now, we are in the position of solving the beamforming optimization sub-section. To approximate the non-convex parts iteratively, we introduce a new auxiliary variable $\Upsilon>0$ which satisfies the constraint

$$(\|\mathbf{W}_1\|^2 + \|\mathbf{W}_2\|^2)\epsilon^{-1} + P_{\sum}^{crt} \le \Upsilon. \tag{14}$$

From the optimal value of phase shift obtained by solving Alg. 1, the problem (11) can be re-expressed as

P4: Beamforming

$$\max_{\mathbf{W},\Upsilon} \quad \text{EEM}_{\sum} \triangleq \sum_{n \in \mathcal{N}} \mathcal{R}_n(\mathbf{W})/\Upsilon + \sum_{f \in \mathcal{F}} \mathcal{R}_f(\mathbf{W})/\Upsilon \quad (15a)$$

We introduce another new auxiliary variables $\mathbf{e} \triangleq \{e_n, e_f\}_{n \in \mathcal{N}, f \in \mathcal{F}}$ being soft energy efficiencies and $\gamma \triangleq \{\gamma_n, \gamma_f\}_{n \in \mathcal{N}, f \in \mathcal{F}}$ being SINRs of UE_n and UE_f , respectively. The problem (15) can be rewritten as

$$\max_{\mathbf{W}, \Upsilon, \gamma, e} \text{EEM}_{\Sigma} \triangleq \sum_{n \in \mathcal{N}} e_n + \sum_{f \in \mathcal{F}} e_f$$
 (16a)

s.t.
$$\gamma_n^{x_n}(\mathbf{W}) \ge 1/\gamma_n,$$
 (16b)

$$\gamma_k^{x_k}(\mathbf{W}) \ge 1/\gamma_k,\tag{16c}$$

$$\ln(1+1/\gamma_n)/\Upsilon \ge e_n,\tag{16d}$$

$$\ln(1+1/\gamma_f)/\Upsilon \ge e_f,\tag{16e}$$

$$ln(1+1/\gamma_n) \ge \bar{\mathsf{R}}_n,$$
(16f)

$$\ln(1+1/\gamma_f) > \bar{\mathsf{R}}_f,\tag{16g}$$

To derive a more tractable form, we introduce $\omega \triangleq \{\omega_{n,f} > 0\}_{n \in \mathcal{N}, f \in \mathcal{F}}$ which satisfy the convex constraint $\|\hat{\mathbf{G}}_n \mathbf{W}_{f'}\|^2 \leq \omega_{n,f'}$. Let $x^{(\kappa)}$ represent the feasible point of x at the κ -th iteration of the iterative algorithm. By following Lemmas 1 and 2 in [8], the constraint (16b) can be approximated at the κ -th iteration as

$$\hat{\Xi}_{n,n}(\mathbf{W})/\gamma_n \le f_n^{(\kappa)}(\mathbf{W}_n),\tag{17}$$

where
$$\|\hat{\mathbf{G}}_{n}\mathbf{W}_{n}\|^{2} \geq 2\Re\{(\hat{\mathbf{G}}_{n}\mathbf{W}_{n}^{(\kappa)})^{*}(\hat{\mathbf{G}}_{n}\mathbf{W}_{n})\} - \|\hat{\mathbf{G}}_{n}\mathbf{W}_{n}^{(\kappa)}\|^{2} \triangleq f_{n}^{(\kappa)}(\mathbf{W}_{n}), \quad \hat{\Xi}_{n,n}(\mathbf{W}) \leq \sum_{f \in \mathcal{F}} \left((\Upsilon_{n,f}^{2})/(2\Upsilon_{n,f}^{(\kappa)}) + (\Upsilon_{n,f}^{(\kappa),2})/2\right) + \sum_{n \in \mathcal{N} \setminus \{n\}} \|\hat{\mathbf{G}}_{n}\mathbf{W}_{n}\|^{2} + \sigma_{n}^{2}.$$

By doing the same way like (17), constraint (16c) can be approximated as

$$\Xi_{f,f}(\mathbf{W})/\gamma_f \le f_f^{(\kappa)}(\mathbf{W}_f),$$
 (18)

where
$$\|\hat{\mathbf{G}}_f \mathbf{W}_f\|^2 \ge 2\Re\{(\hat{\mathbf{G}}_f \mathbf{W}_f^{(\kappa)})^*(\hat{\mathbf{G}}_f \mathbf{W}_f)\} - \|\hat{\mathbf{G}}_f \mathbf{W}_f^{(\kappa)}\|^2 \triangleq f_f^{(\kappa)}(\mathbf{W}_f),$$

The function $\ln(1 + 1/\gamma)/\Upsilon$ in left hand side (LHS) of constraints (16d) and (16e) is convex in (γ, Υ) which can be approximated at $(\gamma^{(\kappa)}, \Upsilon^{(\kappa)})$ point as [9, Eq. (18)]

$$\frac{\ln(1+1/\gamma)}{\Upsilon} \ge \frac{2\ln(1+1/\gamma^{(\kappa)})}{\Upsilon^{(\kappa)}} + \frac{1}{\Upsilon^{(\kappa)}(\gamma^{(\kappa)}+1)} - \gamma/(\Upsilon^{(\kappa)}\gamma^{(\kappa)}(\gamma^{(\kappa)}+1)) - \ln(1+1/\gamma^{(\kappa)})\Upsilon/(\Upsilon^{(\kappa)})^{2}$$

$$\triangleq \mathcal{B}^{(\kappa)}(\gamma,\Upsilon), \ \forall \Upsilon^{(\kappa)} > 0, \ \gamma^{(\kappa)} > 0. \tag{19}$$

For the two last constraints (16f) and (16g), they can be approximated as [1, Eq. (34)]

$$\ln(1+1/\gamma) \ge \ln(1+(\gamma^{(\kappa)})^{-1}) + (\gamma^{(\kappa)}+1)^{-1} - \gamma[\gamma^{(\kappa)}(\gamma^{(\kappa)}+1)]^{-1} \triangleq \mathcal{A}^{(\kappa)}(\gamma).$$
 (20)

Based on the explanation above, we can approximate the problem (16) by the following convex problem at iteration $\kappa + 1$:

P5: Convex Problem

$$\max_{\mathbf{W}, \mathbf{\Upsilon}, \mathbf{\gamma}, \mathbf{e}} \quad \text{EEM}_{\sum} \triangleq \sum_{n \in \mathcal{N}} e_n + \sum_{f \in \mathcal{F}} e_f$$
 (21a)

s.t.
$$\|\hat{\mathbf{H}}_n \mathbf{W}_{f'}\|^2 \le \omega_{n,f'}$$
, $\forall n \in \mathcal{N}, f' \in \mathcal{F}$, (21b)

$$\mathcal{B}^{(\kappa)}(\gamma_n, \Upsilon) \ge e_n, \quad \forall n \in \mathcal{N},$$
 (21c)

$$\mathcal{B}^{(\kappa)}(\gamma_f, \Upsilon) \ge e_f, \quad \forall f \in \mathcal{F},$$
 (21d)

$$\mathcal{A}^{(\kappa)}(\gamma_n) \ge \bar{\mathsf{R}}_n, \quad \forall n \in \mathcal{N},$$
 (21e)

$$\mathcal{A}^{(\kappa)}(\gamma_f) \ge \bar{\mathsf{R}}_f, \quad \forall f \in \mathcal{F},$$
 (21f)

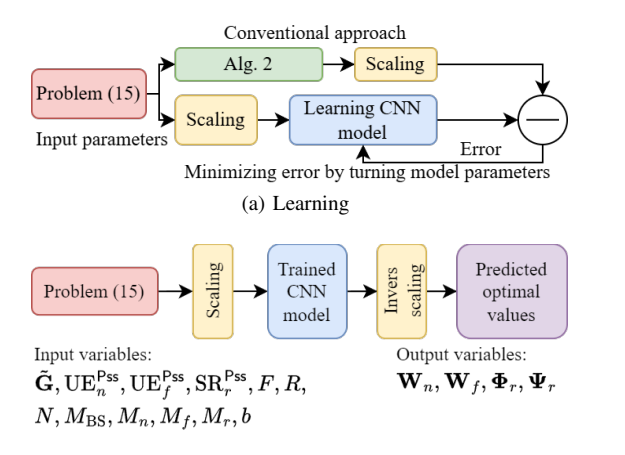
In the end, we can summarize the proposed iterative algorithm with low complexity in Alg. 2 including Alg. 1.

Algorithm 2: Proposed IA Algorithm to Solve Problem (10)

- 1: **Initialization:** Set $(\mathbf{W}, \Phi, \Psi) := 0$, and generate an initial feasible point $(\mathbf{W}^{(0)}, \Upsilon^{(0)}, \gamma^{(0)}, \omega^{(0)})$ randomly;
- 2: Output: EEM_{\sum} and $(\mathbf{W}^{\star}, \mathbf{\Phi}^{\star}, \mathbf{\Psi}^{\star})$.
- 3: repeat
- 4: Find Φ^* and Ψ^* using Algorithm 1;
- 5: Solve problem (21) to achieve $(\mathbf{W}^{\star}, \Upsilon^{\star}, \gamma^{\star}, \omega^{\star})$;
- 6: until Convergence
- 7: Calculate EEM_{\sum} in (10) based on $(\mathbf{W}^{\star}, \mathbf{\Phi}^{\star}, \mathbf{\Psi}^{\star})$;

IV. DEEP LEARNING FRAMEWORK FOR EEM PROBLEM

In this section, we propose a novel DL-based CNN model framework for the EEM problem in multi-STAR-RIS-assisted mMIMO-NOMA networks as illustrated in Fig. 2. As shown in Fig. 2(a), the CNN model learns by off-line the relationship between the input parameter from problem (10) and optimal solution as target variables, which is achieved from Alg. 2. The scaling function is applied to standardize input data between 0 and 1, ensuring stable gradient flow and faster convergence of the CNN model. After completing the learning process, the trained deep CNN model comprising weights and biases can be utilized to predict the optimal precoding



(b) Predicting
Fig. 2. The proposed DL-based CNN framework to the EE problem

matrix and the phase shift at the STAR-RISs whenever new input parameters become available at the input model in realtime with high accuracy as shown in Fig. 2(b). Contrasting the conventional approach, the formulated problem must be addressed by Alg. 2 to achieve the optimal solutions of the phase shift of transmission/reflection at the STAR-RISs and the precoding matrix. In the proposed DL framework, we consider small-scale fading $\tilde{\mathbf{G}}$, position of all users $\{\mathrm{UE}_n^{\mathsf{Pss}}, \mathrm{UE}_f^{\mathsf{Pss}}\}$, position of all STAR-RISs SR_r^{Pss} , the number of far users F, the number of STAR-RISs R, the number of near users N, the number of antennas at BS $M_{\rm BS}$, the number of antennas at users $\{M_n, M_f\}$, the number of elements at STAR-RIS M_r and the number of bits quantization b as the input parameters of CNN model to predict precoding matrix of near user W_n , the precoding matrix of far user \mathbf{W}_f and phase shift of transmission and reflection at STAR-RIS $\{\Psi_r, \Phi_r\}$ as output parameters. Thus, the input dimension of the CNN model is $R(M_r \times M_{\rm BS}) + N(M_n \times M_{\rm BS})(M_n \times M_r/2) + F(M_f \times M_r/2)$ $M_r/2$) + 2N + 2F + 2R + 8, while the output dimension is $(N+F)(M_{\rm BS}\times d)+RM_r$. The scaling is also applied in the predicting phase to normalize the input data for the CNN model, while inverse scaling restores the predicted values to their original scale for accurate results.

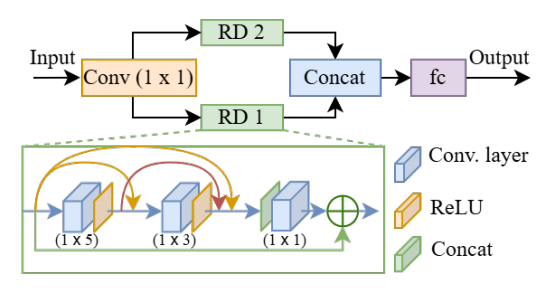


Fig. 3. The architecture of the Deep CNN design.

Fig. 3 illustrates the proposed model architecture of the deep CNN design, where the deep CNN model is developed with two main residual dense (RD) parallel-connected blocks. These blocks are designed to effectively capture input

deeper features by establishing multi-level connections among feature maps. Each RD block is configured with multiple convolutional layers, ensuring enhanced feature extraction and efficient gradient flow. Within the RD blocks, the 1×1 dimensional convolution layer is applied to reduce dimensionality while preserving essential features. The outputs from various layers are aggregated using a concatenation (concat) layer, ensuring a comprehensive fusion of features at different processing stages. The fully connected (fc) layer transforms the extracted features into the final prediction space. Dense connections within the RD blocks mitigate the vanishing gradient problem, accelerate convergence, and enable more effective learning. Additionally, the use of multiple RD blocks addresses potential overfitting, fostering better generalization. This design ensures that the model provides accurate and efficient predictions, even in real-time applications, by leveraging the strengths of residual dense learning and feature aggregation. Moreover, we used the rectified linear unit (ReLU) as an activation function while all convolution and fc layers were configured with 64 kernels and neurons, respectively.

V. SIMULATION RESULTS

To demonstrate the performance of the proposed algorithms in solving the formulated problem in multi-STAR-RISs-assited mMIMO-NOMA networks, we set the simulation parameters as follows: cell dimension 500 m \times 500 m, $\bar{\rm R}_n = \bar{\rm R}_f = 1$ bps/Hz, $d_1 = 200$ m, $d_2 = 100$ m, $M_n = M_f = 10$, $P_{\rm BS}^{dyn} = 10$ dBm, $P_{\rm BS}^{stat} = 15$ dBm, and $P_n^{stat} = P_f^{stat} = 5$ dBm. The convex problem is solved using the SDPT3 solver and the YALMIP toolbox within the MATLAB environment [1]. A dataset is generated with a ratio of 90:10, which is used for training and testing, respectively.

Fig. 4(a) demonstrates the effectiveness of Alg. 2 in solving problem (10) under varying maximum power budgets and number of BS antennas. The Alg. 2 converges to the optimal values within 10 iterations by consistently finds improved solutions in each iteration. As the maximum power budget increases, the average EE also improves, reflecting the proportional relationship between EE performance and SE, as defined by the objective function (15a). Additionally, increasing the number of BS antennas further enhances the average EE by leveraging the higher degrees of freedom (DoF) available in the network.

Fig. 4(b) shows the impact of the epoch on the root mean square error (RMSE) with a variation datasets. As depicted in Fig. 4(b), the RMSE decreases as the number of epochs increases due to the DL model refining its weights and biases throughout the learning process. The proposed CNN model achieves the lowest RMSE, surpassing the DNN model [6], demonstrating its superior ability to approximate high-dimensional datasets. Furthermore, all models (DNN and CNN) trained with a larger dataset outperform the one trained with a smaller dataset, as it can learn more features and patterns from the additional data.

Fig. 4(c) illustrates the average EE as a function of the number of STAR-RISs K with varying numbers of STAR-

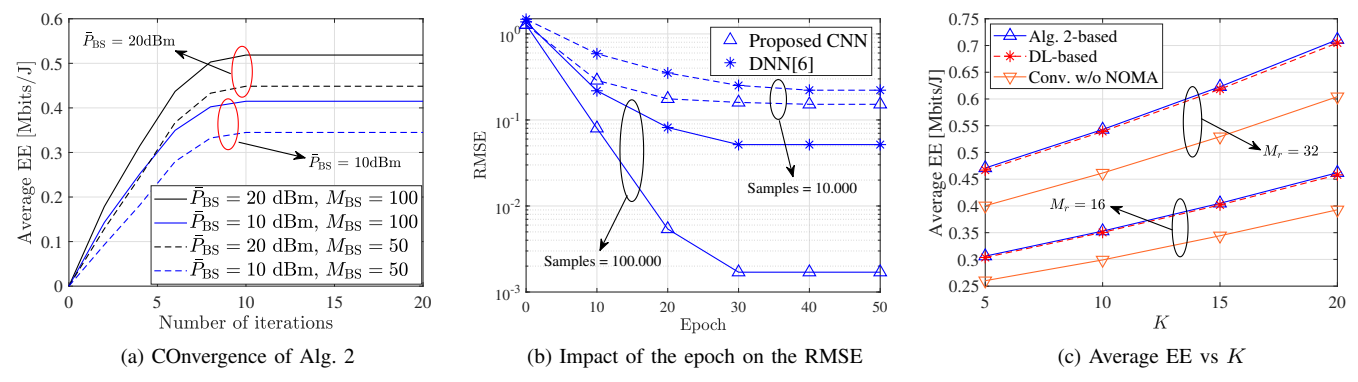


Fig. 4. Convergence of Alg. 2, RMSE versus epoch and impact of K on the average EE

RIS elements. As the number of STAR-RISs increases, the average EE improves due to the enhanced signal quality at the users. Similarly, increasing the number of STAR-RIS elements further boosts the average EE since it allows the system to better focus the desired signal toward the users. Moreover, the conventional without (w/o) NOMA is the worst performer since it requires separate time-frequency resources for each user. Additionally, the DL-based approach accurately predicts the optimal precoding matrix and phase shifts at the STAR-RIS, enabling it to achieve strong EE performance.

Number of UEs	Alg. 2-based	DL-based
8	52.3 s	0.0127 s
12	78.6 s	0.0129 s
16	102.1 s	0.0131 s

In the end, we evaluate the execution time of the DL-based approach in obtaining the optimal solution as shown in Table I. The results indicate that the DL-based approach achieves the optimal solution with a less execution time, even as the number of users increases. In contrast, the Alg. 2-based approach takes significantly longer as the number of users grows. The reason is that the DL-based approach leverages a mapping function to directly predict the optimal value, whereas the Alg. 2-based approach requires multiple iterations to obtain the optimal solution, resulting in higher execution time.

VI. CONCLUSIONS

This paper studied DL-based EEM in STAR-RISs-assisted mMIMO-NOMA networks. We formulated the problem of jointly optimizing the precoding matrix and STAR-RIS phase shifts to maximize energy efficiency, subject to the BS's power budget, STAR-RIS phase shift constraints, and minimum QoS requirements belonging to the mixed-integer programming class. To address this problem, we decoupled it into two sub-problems, phase shift, and beamforming optimization, addressing them separately. For phase shift optimization, we employed a bisection search algorithm, while the beamforming problem was transformed into a more tractable non-convex form and solved using an IA based on the inner approximation

method. To enable real-time optimization, we designed a DL framework to predict optimal phase shifts and precoding matrices under various parameter settings. Simulation results demonstrated that the DL-based approach accurately predicted optimal solutions and performed significantly faster than conventional methods. We also evaluated the impact of essential parameters on the system's performance.

ACKNOWLEDGMENT

The work of T.-V. Nguyen and D. H. N. Nguyen was supported by the U.S. National Science Foundation under grants ECCS-2146436 and CCF-2322190. The work of R. H. Y. Perdana, Y. Pramitarini, and B. An was supported by National Research Foundation of Korea (NRF) grant funded by the Korea government (MSIT) (NRF-2022R1A2B5B01001190). Prof. Beongku An is the corresponding author.

REFERENCES

- R. H. Y. Perdana, T.-V. Nguyen, and B. An, "Adaptive User Pairing in Multi-IRS-aided Massive MIMO-NOMA Networks: Spectral Efficiency Maximization and Deep Learning Design," *IEEE Trans. Commun.*, vol. 71, no. 7, pp. 4377–4390, 2023.
- [2] L. You, Y. Huang, D. Zhang, Z. Chang, W. Wang, and X. Gao, "Energy Efficiency Optimization for Multi-Cell Massive MIMO: Centralized and Distributed Power Allocation Algorithms," *IEEE Trans. Commun.*, vol. 69, no. 8, pp. 5228–5242, 2021.
- [3] Y. Zhao, I. G. Niemegeers, and S. M. De Groot, "Dynamic Power Allocation for Cell-Free Massive MIMO: Deep Reinforcement Learning Methods," *IEEE Access*, vol. 9, pp. 102 953–102 965, 2021.
- [4] M. Soltani, V. Pourahmadi, A. Mirzaei, and H. Sheikhzadeh, "Deep Learning-Based Channel Estimation," *IEEE Commun. Lett.*, vol. 23, no. 4, pp. 652–655, 2019.
- [5] Q. Wu and R. Zhang, "Towards Smart and Reconfigurable Environment: Intelligent Reflecting Surface Aided Wireless Network," *IEEE Commun. Mag.*, vol. 58, no. 1, pp. 106–112, nov 2020.
- [6] R. H. Y. Perdana, T.-V. Nguyen, and B. An, "A Deep Learning-Based Spectral Efficiency Maximization in Multiple Users Multiple STAR-RISS Massive MIMO-NOMA Networks," in 2023 Twelfth Int. Conf. Ubiquitous Futur. Networks. Paris, France: IEEE, 2023, pp. 675–680.
- [7] Q. Wu and R. Zhang, "Beamforming Optimization for Wireless Network Aided by Intelligent Reflecting Surface with Discrete Phase Shifts," *IEEE Trans. Commun.*, vol. 68, no. 3, pp. 1838–1851, Mar. 2020.
- [8] T. V. Nguyen, V. D. Nguyen, D. B. Da Costa, and B. An, "Hybrid User Pairing for Spectral and Energy Efficiencies in Multiuser MISO-NOMA Networks with SWIPT," *IEEE Trans. Commun.*, vol. 68, no. 8, pp. 4874–4890, Aug. 2020.
- [9] V. D. Nguyen, H. V. Nguyen, O. A. Dobre, and O. S. Shin, "A New Design Paradigm for Secure Full-Duplex Multiuser Systems," *IEEE J. Sel. Areas Commun.*, vol. 36, no. 7, pp. 1480–1498, 2018.